Tonkie Khimicheskie Tekhnologii = Fine Chemical Technologies.
2026;21(1):73–89
ISSN 2686-7575 (Online)

Synthesis and processing of polymers and polymeric composites

Синтез и переработка полимеров и композитов на их основе

UDC 691.175.743, 678.074
https://doi.org/10.32362/2410-6593-2026-21-1-73-89
EDN BDSWGG

RESEARCH ARTICLE

The use of nitrile butadiene rubber in the composition of intumescent fire-retardant materials based on plasticized polyvinyl chloride

Andrey A. Galiguzov✉, **Nikolay V. Yashin, Viktor V. Avdeev**

Lomonosov Moscow State University, Faculty of Chemistry, Moscow, 119991 Russia

✉ *Corresponding author, e-mail: agaliguzov@yandex.ru*

Abstract

Objectives. To investigate the properties of intumescent fire-retardant materials based on plasticized polyvinyl chloride and oxidized graphite as functions of their content of nitrile butadiene rubber.

Methods. Intumescent fire-retardant materials with different contents of nitrile butadiene rubber (from 0 to 20 wt %) were obtained. The materials were prepared in the form of a sheet 38–52 mm wide and 1.5–1.9 mm thick by means of flat-die extrusion using a twin-screw compounding extruder. The raw materials used were plasticized polyvinyl chloride with a K-value of 71, nitrile butadiene rubber with a bound acrylonitrile content of 31–35%, oxidized graphite, and ultrafine aluminium hydroxide. The properties of the raw materials and the resulting fire-retardant materials were investigated using infrared spectroscopy, thermal analysis, scanning electron microscopy, as well as mechanical tests, flammability tests, and thermal shock foaming tests.

Results. The mechanical, thermal, and fire-retardant properties of the obtained materials were studied as functions of their contents of nitrile butadiene rubber. The dynamics of foaming in the temperature range from 300 to 800°C were also explored. The flammability rating was determined. The dependence of fire-retardant properties on the melt viscosity of fire-retardant materials was described. The thermal properties were found to be in the temperature range of 40 to 900°C.

Conclusions. The study found that the introduction of nitrile butadiene rubber into fire-retardant materials leads to a change in a number of properties: a decrease in density and hardness; a decrease in tensile strength; an increase in relative elongation; an increase in melt viscosity by 16 times; and, accordingly, a decrease in foaming rate by a factor of 1.43–1.65. It was established that the foaming rate has a linear dependence on the viscosity of the melt of fire-retardant materials. The introduction of rubber leads to an increase in the strength of foamed char by a factor of 4.8. Thermal analysis showed that increasing the rubber content leads to an increase in heat resistance from 222 to 236°C, and resistance to oxidation of foamed graphite in the composition of foamed char from 601 to 659°C. The presence of rubber does not have a noticeable effect on flammability. The established flammability rating for all compositions is V-0.

Keywords

fire-retardant material, oxidized graphite, intumescent material, polyvinyl chloride, plasticizer, foaming rate, tensile strength, flammability, melt flow index

Submitted: 02.07.2025
Revised: 29.11.2025
Accepted: 19.01.2026

For citation

Galiguzov A.A., Yashin N.V., Avdeev V.V. The use of nitrile butadiene rubber in the composition of intumescent fire-retardant materials based on plasticized polyvinyl chloride. *Tonk. Khim. Tekhnol. = Fine Chem. Technol.* 2026;21(1):73–89. https://doi.org/10.32362/2410-6593-2026-21-1-73-89

НАУЧНАЯ СТАТЬЯ

Использование бутадиен-нитрильного каучука в составе интумесцентных огнезащитных материалов на основе пластифицированного поливинилхлорида

А.А. Галигузов✉, Н.В. Яшин, В.В. Авдеев

Московский государственный университет им. М.В. Ломоносова, Химический факультет, Москва, 119991 Россия

✉ *Автор для переписки, e-mail: agaliguzov@yandex.ru*

Аннотация

Цели. Исследование свойств интумесцентных огнезащитных материалов на основе пластифицированного поливинилхлорида и окисленного графита в зависимости от содержания в них бутадиен-нитрильного каучука.

Методы. В настоящей работе были получены интумесцентные огнезащитные материалы с различным содержанием бутадиен-нитрильного каучука (от 0 до 20 мас. %). Материалы были изготовлены в виде полотна шириной 38–52 мм и толщиной 1.5–1.9 мм методом плоскощелевой экструзии с использованием двушнекового экструдера-компаундера. В качестве сырья были использованы пластифицированный поливинилхлорид с константой Фикентчера, равной 71, бутадиен-нитрильный каучук с содержанием связанного акрилонитрила 31–35%, окисленный графит и ультрадисперсный гидроксид алюминия. Свойства сырья и полученных огнезащитных материалов были исследованы методами инфракрасной спектроскопии, термического анализа, сканирующей электронной микроскопии, а также при помощи механических испытаний, испытаний на воспламеняемость и вспенивание при термоударе.

Результаты. Представлены результаты исследований механических, термических и огнезащитных свойств полученных материалов в зависимости от содержания в них бутадиен-нитрильного каучука. Определена динамика вспенивания в температурном интервале от 300 до 800°C. Определена группа воспламеняемости. Приведена зависимость огнезащитных свойств от вязкости расплава огнезащитных материалов. Определены термические свойства в температурном интервале от 40 до 900°C.

Выводы. В исследовании установлено, что введение бутадиен-нитрильного каучука в огнезащитные материалы приводит к изменению ряда свойств: снижению плотности и твердости, снижению прочности на растяжение, увеличению относительного удлинения, росту вязкости расплава в 16 раз и, соответственно, снижению степени вспенивания в 1.43–1.65 раз. Установлено, что степень вспенивания имеет линейную зависимость от вязкости расплава огнезащитных материалов. Введение каучука приводит к повышению прочности пенококса в 4.8 раз. Термический анализ показал, что увеличение содержания каучука приводит к росту термостойкости с 222 до 236°C и стойкости к окислению вспененного графита в составе пенококса с 601 до 659°C. Наличие каучука не оказывает заметного влияния на воспламеняемость. Установлена группа воспламеняемости для всех составов — V-0.

Ключевые слова

огнезащитный материал, окисленный графит, интумесцентный материал, поливинилхлорид, пластификатор, степень вспенивания, прочность при растяжении, воспламеняемость, показатель текучести расплава

Поступила: 02.07.2025
Доработана: 29.11.2025
Принята в печать: 19.01.2026

Для цитирования

Галигузов А.А., Яшин Н.В., Авдеев В.В. Использование бутадиен-нитрильного каучука в составе интумесцентных огнезащитных материалов на основе пластифицированного поливинилхлорида. *Тонкие химические технологии*. 2026;21(1):73–89. https://doi.org/10.32362/2410-6593-2026-21-1-73-89

INTRODUCTION

Fire protection is currently a pressing issue for most of the infrastructure of public utilities and various industries. During a fire, structures and facilities are subject to significant loads which can lead to severe damage and cause colossal losses to the national economy. This issue is addressed by using passive fire protection materials based on various polymers and fire retardants, such as paints, enamels, impregnations, pastes, tapes, profiles, *inter alia* [1]. In recent years, fire protection tapes and profiles based on polyvinyl chloride (PVC) and expandable graphite have found widespread use [2–6]. Their applications include fire sleeves and fire-retardant materials (FRMs) for fire doors, windows, ventilation boxes and ducts, and elevators in civil and industrial facilities. Under thermal shock conditions, such materials foam repeatedly to form a non-combustible foamed char, filling process openings and gaps. The foam acts as a thermal barrier, and prevents flame spread. The effectiveness of intumescent FRMs depends on a combination of factors: the thickness of the foamed char; the foaming rate; and the properties of the foamed char (structure, chemical composition, cross-linking density, mechanical strength, viscoelastic properties, density, porosity, thermal conductivity, etc.). Under fire conditions, the resulting foamed char is subject to mechanical stress (stretching, compression, shear, impact loads) due to various factors: expansion of metal structural parts under the influence of heat flow, vibration, physical contact with various objects (due to falling objects during a fire), and the action of turbulent flows [7]. In this regard, one of the most important characteristics is the mechanical strength of the foamed char, both under maximum operating temperatures and during fire dynamics.

The use of PVC as a polymer base in intumescent FRMs is an important trend in the development of passive fire protection products. However, PVC itself is a rigid polymer. The use of plasticizers allows the final material to acquire the desired properties such as: elasticity, flexibility, and frost resistance. Plasticized materials have a lower viscosity, allowing for lower processing temperatures, a higher degree of filling, and higher homogeneity of mixture [8]. However, the disadvantages of such polymer materials (PMs) include a low oxygen index (LOI) (up to 19–22%) and high smoke generation [9], as well as low durability due to the presence of a low-molecular-weight plasticizer, which can migrate to the product surface [10]. The use of high-molecular-weight plasticizers can mitigate or, in some cases, completely eliminate these disadvantages [11].

Several studies [12–15] have demonstrated the compatibility of PVC with nitrile butadiene rubber (NBR). PMs based on these components have been available as commercial products for the past 80 years [16]. PVC and NBR have been shown [17] to be compatible in any ratio at an acrylonitrile content in the rubber of 23–45%. The introduction of NBR into PVC allows for PMs to be obtained with properties characteristic of elastomers: increased resistance to oils and solvents; high tensile strength; abrasion resistance; bending resistance; increased residual deformation under compression and resistance to plasticizer migration; and loss of volatiles. For example, replacing half of the low-molecular-weight plasticizer dioctyl phthalate (DOP) with NBR in PVC plasticate leads to an increase in tensile strength by 25%, an increase in relative elongation by 6%, and a decrease in plasticizer migration from 3 to 0.5%. Complete replacement of the low-molecular-weight plasticizer with NBR is impossible, since a plasticizing effect is observed only at an NBR content of 30%. Such mixtures are not always convenient for processing and filling due to the high melt viscosity [15].

PMs based on NBR and plasticized PVC are characterized by high thermal stability. For complex material, this parameter is higher than that for NBR due to the lower fraction of double bonds in the mixture and the presence of chlorine.

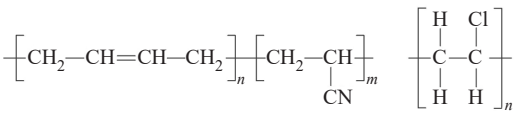

Fig. 1. Structural formulas of NBR (left) and PVC (right)

Thermal oxidation of NBR is a single-stage process. It begins to degrade at 360°C [18]. In the range of 360–500°C, the polymer chain ruptures to release degradation products. These are polymer chain constituents: polybutadiene and polyacrylonitrile, as well as products of the interaction of diene fragments with the nitrile group [19, 20]. This is the range with the highest weight loss: 87.7% [20]. Pyrolysis takes place in the temperature range above 600°C with formation of butadiene, acrylonitrile, benzene, 1,4-cycloheptadiene, 4-vinylcyclohexene, benzonitrile, and other saturated cyclic products [21]. At temperatures up to 900°C, NBR completely degrades, leaving almost no carbon residue.

Thermal and thermo-oxidative degradation of PVC is a more complex process. Pure PVC begins to

degrade at a temperature of 250°C. This stage occurs in the temperature range of 250–350°C, accompanied by a dehydrochlorination reaction with a weight loss of up to 65%. In addition to hydrochloric acid, the degradation products are benzene, toluene, and other unsaturated cyclic hydrocarbons. In the second stage (350–525°C), the dehydrochlorinated residues undergo cracking and degradation to release polyene chains [22]. In the case of plasticized PVC, the low-molecular-weight plasticizer evaporates in the first and second stages. For individual substances, the boiling points are as follows: for DOP, 380°C; for diisononyl phthalate, 252°C, for dioctyl terephthalate, 400°C; and for the plasticizer in the PM, the weight loss temperatures shift to higher temperatures [23]. At temperatures above 525°C, polyene chains degrade to toluene and other low-molecular-weight alkylbenzenes. At temperatures up to 900°C, the yield of carbon residue ranges from 5 to 10% [24, 25].

Thermal degradation of PVC–NBR blends is a two-stage process. In the first and second stages of degradation, the weight loss is lower than for the individual components. The yield of carbon residue at 600°C is 3–4 times higher than that for PVC and NBR. The weight loss curves are not additive with respect to the components of the blend. The degradation products are dominated by low-molecular-weight substances: toluene, acrylonitrile, butenenitrile, and hydrogen cyanide [20]. The increase in the yield of carbon residue probably results from the formation of free radicals of components of the binary mixture and the interaction of macromolecules to form polycyclic structures.

When inorganic fillers (kaolin, $Mg(OH)_2$) are introduced into the binary mixture, the degradation rate decreases and the degradation maximum shifts to higher temperatures. This is due to the formation of a thermal barrier. The amount of HCl formed by the reaction with the filler also decreases. During degradation, the yield of carbon residue increases non-additively [20]. This phenomenon is also characteristic of both polyolefins and their copolymers [26].

The yield of carbon residue and its mechanical strength are important characteristics for intumescent FRMs. They are critical, especially in the case of a jet fire or the occurrence of turbulent gas flow during the use of intumescent materials under real-life conditions. A high level of hardness and a developed crack structure lead to rapid destruction and ablation of the foamed char. Foamed char with low mechanical strength does not ensure long-term performance under turbulent combustion conditions [7].

The effect of NBR content in intumescent materials based on plasticized PVC and oxidized graphite has not been studied widely. The aim of this study was to investigate the effect of NBR content on the mechanical, thermal, and fire-retardant properties of intumescent FRMs based on plasticized PVC and oxidized graphite.

EXPERIMENTAL

Materials

Intumescent FRMs of various compositions were studied, obtained from the following components:

Component 1: suspension PVC (*SIBUR Holding*, Russia), 271PC grade, the Fikentscher constant K = 71.0 ± 1.0, bulk density 0.46–0.57 g/cm^3, TU 20.16.30-001-83385954-2018;

Component 2: DOP (*VitaKhim*, Russia), premium grade, GOST 8728-88[1];

Component 3: RITMIKS-2040/2 complex lead-based stabilizer (*SKhK*, Russia), TU 20.59.56-020-21996423-2020;

Component 4: NBR powder (*SIBUR Holding*), PBNK-3365 grade, bound acrylonitrile content 31–35%, Mooney viscosity (ML 1+4 at 100°C) 65 MU, TU 38.30328-2008;

Component 5: ultrafine aluminum hydroxide $Al(OH)_3$, TS 303 grade, D50 3–6 μm, moisture content 0.3%, loss on ignition 33.0–34.5%, aqueous suspension pH 9.2, pycnometric density 2.401 g/cm^3, TU 2322-001-23374430-2015;

Component 6: stearic acid (China), SA1860 grade;

Component 7: oxidized bisulfate graphite (*Ningbo Borhe,* China), EG-250 grade, expansion volume 250 cm^3/g, foam graphite yield 65%, moisture content 0.5%, aqueous extract pH 2.9, pycnometric density 1.587 g/cm^3, particle size composition—see Table 1.

Methods

The materials were produced by a three-stage process.

Stage 1. In the first stage, PVC plasticate powder was obtained by mixing components 1–3 in a weight ratio of 100 : 70 : 6 (final mixing temperature 110°C). The plasticate was then conditioned at 18–25°C for 24 h.

Stage 2. In the second stage, five samples with varying NBR contents were produced by mixing the PVC plasticate powders and components 4–7. In all cases, the total polymer content (PVC plasticate + NBR) was the same, 60 wt %. Within this total content, the NBR content was varied so that the NBR content

[1] GOST 8728-88. Interstate Standard. Plasticizers. Specifications. Moscow: IPK Izdatelstvo standartov; 1990 (in Russ.).

Table 1. Particle size composition (wt %) of oxidized bisulphate graphite, EG-250 grade (mm)

Particle size, mm	+1.0	−1.0 + 0.63	−0.63 + 0.4	−0.4 + 0.315	−0.315 + 0.2	−0.2 + 0.16	−0.16 + 0.1	−0.1 + 0.05	−0.05
Content, %	0	0	0.5	1.7	54.8	27.4	0.1	13.9	1.5

Table 2. Composition (wt %) of PMs and FRMs with various NBR contents

Material code	Component						
	PVC	DOP	Stabilizer	Stearic acid	NBR	$Al(OH)_3$	Oxidized graphite
PM-0	56.72	39.59	3.40	0.29	0	0	0
PM-5	51.88	36.32	3.11	0.29	8.40	0	0
PM-10	47.21	33.05	2.83	0.29	16.62	0	0
PM-15	42.47	29.72	2.55	0.29	24.97	0	0
PM-20	37.76	26.44	2.27	0.29	33.24	0	0
FRM-0	34.06	23.84	2.04	0.18	0	9.88	30
FRM-5	31.22	21.85	1.87	0.18	5.00	9.88	30
FRM-10	28.37	19.87	1.70	0.18	10.00	9.88	30
FRM-15	25.54	17.87	1.53	0.18	15.00	9.88	30
FRM-20	22.70	15.88	1.36	0.18	20.00	9.88	30

in the final composition was 0, 5, 10, 15, and 20 wt %. The total aluminum hydroxide and oxidized graphite contents were the same in all compositions (10 and 30%, respectively). In order to evaluate the dynamics of the properties of PMs upon the introduction of fire retardants, five polymer samples were also obtained. They contained no fire retardants and the weight ratio between PVC and NBR remained the same. Table 2 presents the compositions of the resulting mixtures.

Stage 3. In the third stage, each of the mixtures obtained (FRM and PM) was extruded by a twin-screw extruder with corotating screws (D_S = 20 mm and L_S/D_S = 44. D_S and L_S are the extruder screw diameter and length, respectively) at a temperature of 165–170°C and a screw speed of 170 rpm using a T-shaped flat die. During extrusion, the screw motor load was recorded as a percentage of the maximum value. A two-roll calender with water-cooled rolls was used to form a sheet. Thus, for each composition, a sheet 38–52 mm wide and 1.5–1.9 mm thick was obtained. The characteristics of the resulting materials were determined using a number of methods.

RESEARCH METHODS

Composition of fire retardants

The study ascertained the pHs of the aqueous suspension (for aluminum hydroxide, according to GOST 21119.3-91[2]) and aqueous extract (for oxidized graphite, according to GOST 17818.6-90[3]) of the fire retardants.

[2] GOST 21119.3-91. Interstate Standard. General methods of test for pigments and extenders. Determination of pH value of an aqueous suspension. Moscow: IPK Izdatelstvo standartov; 1999 (in Russ.).

[3] GOST 17818.6-90. State Standard of the USSR. Graphite. Method for determination of hydrogen ions concentration of water suspension and water extract. Moscow; 1990 (in Russ.).

The composition of the fire retardants was analyzed using a TENSOR 27 FTIR spectrometer (*Bruker*, Germany) with a DLaTGS detector in the 4000–400 cm^{-1} range with a resolution of 4 cm^{-1} using pellets of alkali metal halides (KBr) with $Al(OH)_3$ or oxidized graphite in ratios of 1 : 500 and 1 : 850, respectively.

Density and hardness

The density D and Shore A hardness H_A of the materials obtained (PMs and FRMs) were determined according to GOST 15139-69[4] and GOST 24621-2015[5], respectively.

Melt flow index (MFI)

In the case of FRMs, MFI was measured according to GOST 11645-2021[6] using an XNR-400 analytical plastometer at a temperature of 190°C and a load of 5.0 kg.

Tensile strength

In the case of the PM and FRM samples, the tensile strength σ_t and relative elongation ε_t were determined according to GOST 270-75[7]. The test was conducted at room temperature on Type II specimens (detailed notations and dimensions are specified in the regulatory documentation GOST 270-75) using an HxK-S/U series universal testing machine, modification H5K-S (*Tinius Olsen*, United Kingdom) at a travel speed of (500 ± 50) mm/min.

Thermal properties

The thermal properties of the raw materials, PMs, and FRMs were determined using dynamic thermogravimetric analysis in an air atmosphere (60 cm^3/min) using an STA 449 simultaneous thermal analyzer (*Netzsch*, Germany) in the temperature range of 40–900°C at a temperature increase rate of 20 K/min. Based on the results of thermal analysis, thermal stability was found from the onset degradation temperature T_i , and the temperature T_{max} of the maximum decomposition rate [5].

Foaming rate

The foaming rate *FR* of the FRM samples was determined as a function of the specified isothermal holding temperature. The test was conducted in air using the method described in GOST R 59637-2021[8]. FRM samples with a diameter of 40 ± 0.5 mm, and an actual initial thickness T_0 measured with a caliper, were placed in a hollow steel cylinder with a diameter of 41 mm and a height of 60 mm. Next, the steel cylinder containing the sample was mounted on a steel support and then placed in a muffle furnace preheated to the specified temperature. After 5 min, the steel cylinder was removed from the furnace and cooled to room temperature. The test was performed in triplicate for each sample. The heights T_0 and T_1 of the initial and foamed samples, respectively, were measured with a caliper.

The foaming rate was determined at temperatures ranging from 300 to 800°C in 100°C increments. The foaming rate *FR* was calculated using the following equation

$$FR = [(T_1 - T_0)/T_0] \times 100\%.$$

The foaming dynamics was determined for each FRM as a function of the specified holding temperature.

The sample heating rate was determined for each preset furnace temperature from 300 to 800°C. A thermocouple was installed at the sample location to record the temperature over a period of up to 5 min (Fig. 2).

As can be seen in Fig. 2, the higher the preset furnace temperature, the higher the sample heating rate v_0 at the initial time. Temperature is known to be a key factor in the foaming process of expandable graphite: with increasing temperature, the foaming rate increases and the bulk density of the expanded graphite decreases [27].

4 GOST 15139-69. State Standard of the USSR. Plastics. Methods for the determination of density (volume mass). Reprint, February, 1988, with correction 1. Moscow: IPK Izdatelstvo standartov; 1999 (in Russ.).

5 GOST 24621-2015. Interstate Standard. Plastics and ebonite. Determination of indentation hardness by means of a durometer (Shore hardness). Moscow: Standartinform; 2015 (in Russ.).

6 GOST 11645-2021. Interstate Standard. Plastics. Methods for determination of flow index of thermoplastics melt. Moscow: Russian Standardization Institute; 2025 (in Russ.).

7 GOST 270-75. Interstate Standard. Rubber. Method of the determination elastic and tensile stress-strain properties. Moscow: Standartinform; 2008 (in Russ.).

8 GOST R 59637-2021. National Standard of the Russian Federation. Fire protection means for buildings and structures. Means of fire protection. Methods of quality control of fire-retardant works during installation (application), maintenance and repair. Moscow: Russian Standardization Institute; 2021 (in Russ.).

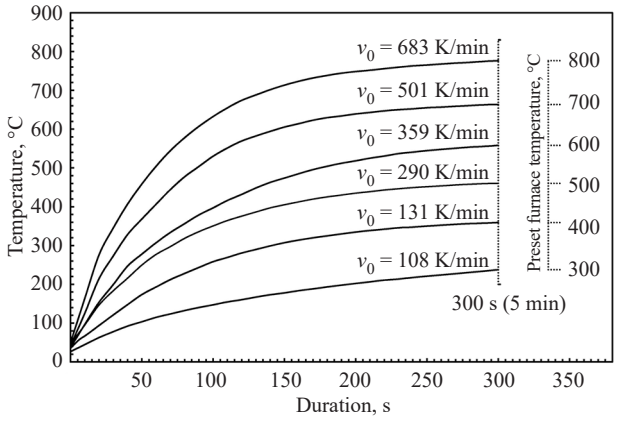

Fig. 2. Dependence of the temperature of a FRM sample on the duration of holding at a preset furnace temperature

Mechanical strength of foamed char

In the case of the FRM samples foamed at 600°C, the mechanical strength σ_f of the foamed char was determined according to a published procedure [28]. The foamed char sample was placed between two horizontal plates secured to the crosshead of a testing machine. The test was conducted at room temperature using an HxK-S/U universal testing machine, modification H5K-S, at a travel speed of 2.5 mm/min with a force meter accuracy of ±2.5 N. Each sample was tested in such a way that the final distance between the plates was 2 mm. Since foamed char produced from such FRMs has a gradient structure and its upper and middle parts have the highest porosity [6], the calculations were made at 75% deformation (for the lower part of the foamed char sample).

Flammability

The flammability of the FRM samples was determined according to UL-94 "Test for Flammability of Plastic Materials for Parts in Devices and Appliances"[9]. For the purposes of testing, specimens with a length of 125 ± 5 mm, a width of 13.0 ± 0.5 mm, and a thickness of 1.5–1.9 mm were cut from fragments of the extruded FRM sheet. The specimens were then conditioned at a temperature of 23 ± 2°C and a relative humidity of 50 ± 5% for 48 h. All specimens were tested for compliance with the V-0 flammability rating: vertical specimen position, gas burner flame height 20 mm, flame self-extinguishing within 10 s after flame removal, burning droplets not allowed, and afterglow for 30 s. Three replicate specimens were tested in one single test.

Scanning electron microscopy (SEM)

The structure and morphology of the fire-retardant powders and fracture surfaces of the PM and FRM samples were examined using a TESCAN VEGA3 LMU scanning electron microscope (*Tescan Orsay Holding*, Czech Republic) at an accelerating voltage of 20 V.

RESULTS AND DISCUSSION

The FRMs being studied here are often used as elastic profiles and tapes in structures for various purposes. Therefore, their performance attributes are not limited to fire protection characteristics, but also include their physical and mechanical properties. Table 3 presents the results of characterizing the obtained PMs and FRMs.

In this study, we investigated the effect of NBR on density, Shore A hardness, and tensile strength.

In order to assess the effect of fire-retardant properties on the mechanical properties of FRMs, oxidized graphite and aluminum hydroxide were studied by IR spectroscopy. The pH was determined, and fire-retardant particles were examined by SEM. According to the IR spectrum (Fig. 3), oxidized graphite bisulfate, EG-250 grade, has a number of functional groups: O–H (3438 cm^{-1}); carboxyl COOH (1388 cm^{-1}); carbonyl –C=O (1700 cm^{-1}); and aromatic C=C group (1633 cm^{-1}). The presence of several bands in the range from 1050–950 cm^{-1} may be due to the vibrations of the S=O group. Their low intensity is associated with the low concentration of these groups in the oxidized graphite. The band at 1114 cm^{-1} may be attributed to both the vibrations of the oxygen-containing C–O group and the asymmetric vibrations of SO_4^{2-} [29–31]. Hydroxyl groups are located on the surface of the basal layers. The high intensity of the peak at 3438 cm^{-1} suggests that their content is high.

[9] UL 94 BULLETIN-2018 UL Standard for Safety Tests for Flammability of Plastic Materials for Parts in Devices and Appliances. Underwriters Laboratories Inc. (UL). Northbrook, IL. Fifth Edition, Dated October 29, 1996.

Table 3. Properties of the obtained PMs and FRMs

Material code	NBR content	MFI, g/10 min	D, g/cm^3	H_A, c.u.	σ_t, MPa	ε_t, %	σ_f, MPa	Thermal analysis data			UL-94
								T_{onset}, °C	T_{peak}, °C	Residue at 900°C, %	
PM-0	0	35.0	1.236	61	10.9	249.7	–	–	–	–	–
PM-5	8.40	27.7	1.236	59	10.9	355.6	–	–	–	–	–
PM-10	16.62	17.0	1.219	55	10.8	386.1	–	–	–	–	–
PM-15	24.97	8.8	1.175	49	10.6	421.9	–	–	–	–	–
PM-20	33.24	2.9	1.085	41	9.5	465.6	–	–	–	–	–
FRM-0	0	14.6	1.382	77	6.2	152.4	129.2	222	253	9.47	V-0
FRM-5	5.00	9.4	1.423	77	6.0	211.6	315.6	226	254	8.74	V-0
FRM-10	10.00	5.0	1.405	75	5.8	254.8	321.4	228	260	8.80	V-0
FRM-15	15.00	2.9	1.367	73	5.1	314.2	448.4	233	264	8.49	V-0
FRM-20	20.00	0.9	1.350	69	4.6	384.6	615.4	236	264	9.43	V-0

Note: D, density; H_A, Shore A hardness; σ_t, tensile strength; ε_t, relative tensile elongation; σ_f, mechanical strength of foamed char; T_{onset}, onset degradation temperature; T_{peak}, temperature of the maximum degradation rate; and UL-94, flammability rating according to UL-94.

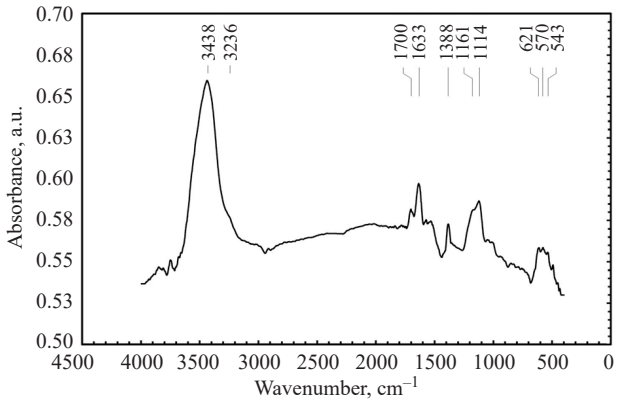

Fig. 3. IR absorption spectra of oxidized bisulphate graphite, EG-250 grade

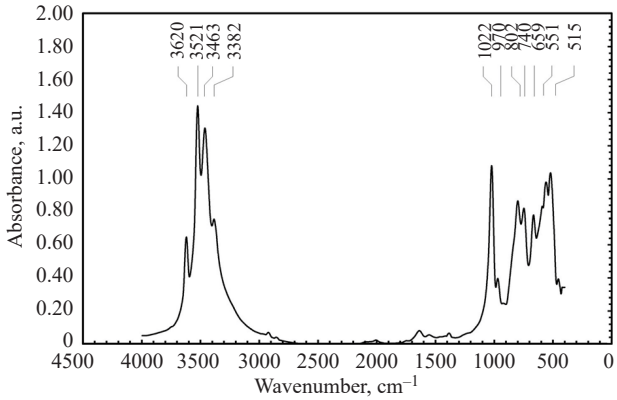

Fig. 4. IR absorption spectra of ultrafine aluminium hydroxide, TS 303 grade

The IR absorption spectrum of ultrafine aluminum hydroxide, TS 303 grade (Fig. 4), shows mainly bands of stretching (in the range from 3620 to 3382 cm^{-1}) and bending (1022 and 970 cm^{-1}) vibrations of the HO group. The bands in the range from 650 to 515 cm^{-1} are assigned to the bending vibrations of the HO group and the vibrations of the AlO group [32].

The fire retardants have different pH values. The pHs of the aqueous extract/suspension are 2.9 and 9.2 for oxidized graphite and aluminum hydroxide, respectively.

Figures 5 and 6 present SEM images of fire-retardant particles.

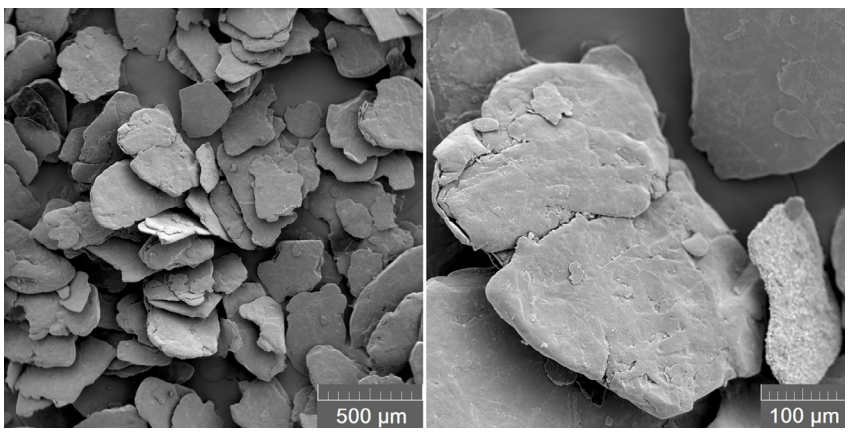

Fig. 5. SEM images of oxidized bisulphate graphite, EG-250 grade

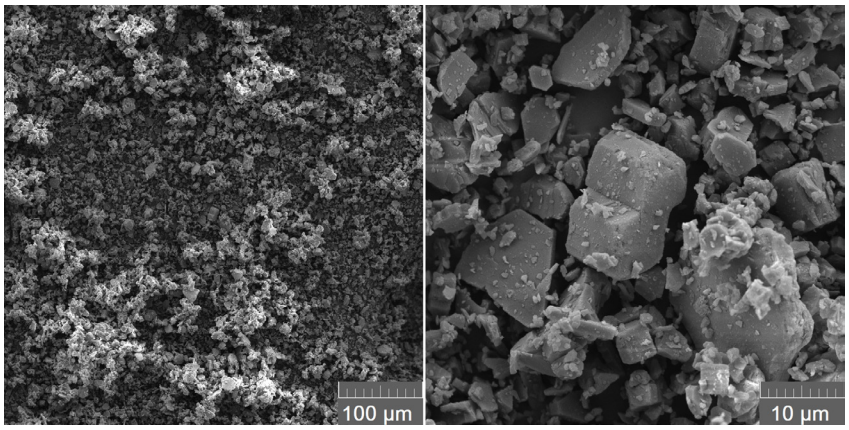

Fig. 6. SEM images of ultrafine aluminium hydroxide, TS 303 grade

As can be seen from Table 3 and Fig. 7, an increase in the NBR content leads to a decrease in density by 12% for PMs. For FRMs, the density remains virtually unchanged (decreases by 2.3%).

The introduction of fire retardants in a given quantity leads to an average increase in density of 12–25%. This is as a result of the addition of denser fillers, the densities of which are 1.587 and 2.401 g/cm^3 for oxidized graphite and aluminum hydroxide, respectively.

An increase in the NBR content leads to a decrease in the Shore A hardness of PMs and FRMs by 33 and 10%, respectively (Fig. 7). These changes are due to the hardness of NBR (49 c.u.) which acts as a high-molecular-weight plasticizer, increasing the mobility of PVC macromolecules, thereby reducing indentation resistance [33]. The introduction of the fire retardants leads to an increase in hardness by a factor of 1.3–1.7. This change is typical of PVC-based PMs with a wide range of fillers at a high degree of filling [34]. In FRMs, the filler strengthens the bonds between macromolecules, hindering their sliding relative to each other. As Fig. 7 shows, the hardness of PMs and FRMs in the range considered changes differently: decreasing by 33 and 10%, respectively. This may be due to the fact that increasing NBR content in FRMs strengthens the bonds between the fillers and the polymer chain units.

Determining the strength characteristics showed that with an increase in the NBR content in PMs and FRMs, the tensile strength σ_t decreases by 13 and 25%, respectively. The relative tensile elongation ε_t increases by a factor of 1.9 and 2.5, respectively. The introduction of the fire retardants leads to a decrease in σ_t and ε_t by a factor of 1.8–2.1 and 1.2–1.7, respectively (Fig. 8).

In the case of PMs, the decrease in σ_t is uneven. In the range up to 15 wt % (based on the FRM composition), this characteristic remains virtually unchanged which is consistent with literature data [13]. However, at a content of 20 wt %, it decreases by 13%.

The effect of fillers on the strength properties of PVC-based PMs has been studied using a wide range of materials. It was noted that the filler is selected based on its compatibility with the PM which depends on the adhesion at the polymer–filler interface [35] and on at least two other factors: the chemical interaction at the interface; and the shape and size of the filler particles.

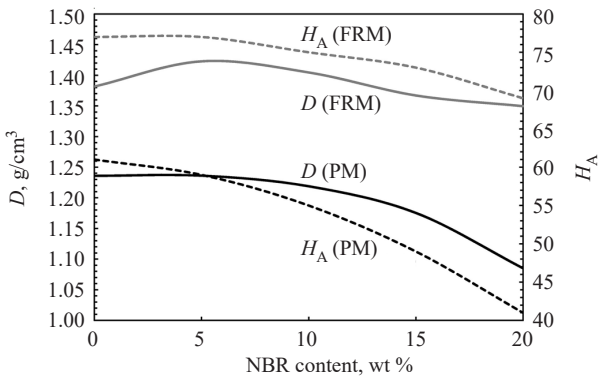

Fig. 7. Dependencies of the density D and Shore A hardness H_A of PMs and FRMs on NBR content

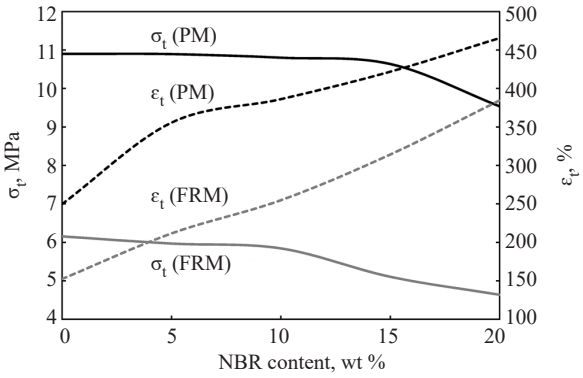

Fig. 8. Dependencies of the density σ_t and relative tensile elongation ε_t of PMs and FRMs on NBR

PVC has weak acidic properties. Its α-hydrogen atoms can form bonds with proton–acceptor substances [36]. A method for increasing interfacial strength is based on increasing the number of hydroxyl groups on the filler surface [37, 38]. At the interface, PVC interacts with basic fillers containing reactive HO groups. Conversely, fillers with pronounced acidic properties exhibit poor compatibility with PVC [37]. According to IR spectroscopy (Fig. 3), a characteristic of oxidized graphite is its high content of surface HO groups. An aqueous extract of this fire retardant is also acidic (pH 2.9). However, it should be noted that the acidity of the aqueous extract is determined by the presence of residual sulfuric acid. Sulfuric acid and hydrosulfate anions are readily washed out of the interlayer space of oxidized graphite by water, passing to solution upon pH determination. However, HO groups are strongly bonded to carbon atoms in the graphite crystal lattice. Overall, based on the peak intensity in the IR spectrum of oxidized graphite, it can be concluded that this fire retardant has basic properties.

Aluminum hydroxide also exhibits basic properties due to the presence of HO groups (Fig. 4). However, despite the apparent chemical compatibility of the materials, the introduction of fire retardants into PMs causes a decrease in their strength properties. The size and shape of the particles are known to affect the properties of PMs under deformation, especially under stretching. Dynamic testing is accompanied by cavitation, i.e., delamination to form cavities near the filler surface [39]. The size of the filler particles determines the formation of defects at the matrix–filler interface in the form of either oval or diamond-shaped pores [40, 41]. The oval pores are created when the filler particle size is up to 100 μm. Such pores do not reduce the mechanical properties. The diamond-shaped pores are formed when the filler particle size is greater than 100 μm; in this case, defects arise that initially grow as oval pores and then transform into diamond-shaped pores. These defects are microcracks growing transversely to the stretching direction. This leads to early failure of the PM. When stretched, the matrix is delaminated along diamond-shaped defects, resulting in a characteristic decrease in strength. It can thus be concluded that, despite the chemical compatibility of fire retardants with the PM, the particle size of oxidized graphite determines the decrease in strength of FRMs.

In this study, we compared the foaming rates of FRMs with different NBR contents, including the dependence on the specified isothermal holding temperature (the sample heating rate, see Fig. 2). The results showed that with an increase in NBR content from 0 to 20%, the foaming rate decreases by a factor of 1.43–1.65. Increasing the holding temperature leads to an increase in the foaming rate of FRMs, which is typical of oxidized graphite [27]. Figure 9 shows that the FRM foaming process can be divided into two stages: 1) before 400°C, when samples of all FRM compositions rapidly foam; and 2) after 400°C, when the foaming is smooth with the sample height changing slightly. In the temperature range of 700–800°C, the sample height decreases because of oxidation of the foamed char. This is especially characteristic of the sample with a large foamed char height, when its upper portion is exposed to an oxidizing environment (sample FRM-0).

Foaming rate is an important parameter of fire protection materials which determines their performance properties. As noted above, rolled FRMs are applied in fire doors, and fire sleeves, inter alia, where one of the fire protection performance characteristics is complete response time which determines the fire resistance limit (GOST R 53306-2009[10]). Figure 9 also shows that NBR

[10] GOST R 53306-2009. National Standard of the Russian Federation. Enclosing building structures crossing junction points by using pipe, which is made of polymeric materials. Fire resistance test. Moscow: Standartinform; 2019 (in Russ.).

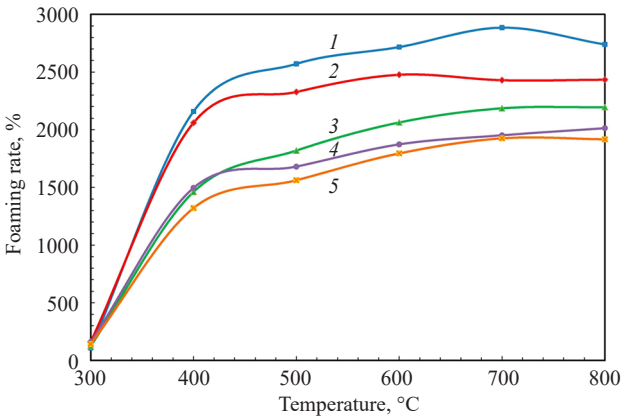

Fig. 9. Dependencies of the foaming rate of FRM on specified isothermal holding temperature at various NBR contents: (*1*) FRM-0, (*2*) FRM-5, (*3*) FRM-10, (*4*) FRM-15, and (*5*) FRM-20

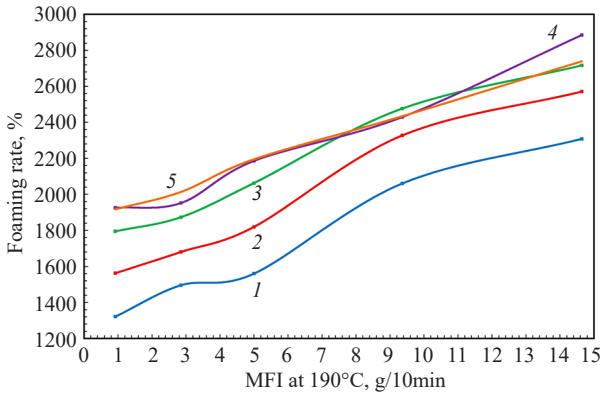

Fig. 10. Dependence of the foaming rate of FRMs on their MFI at different NBR contents and various specified isothermal holding temperatures: (*1*) 400°C, (*2*) 500°C, (*3*) 600°C, (*4*) 700°C, and (*5*) 800°C

content in FRMs affects the maximum foaming rate and foaming speed. Over the entire temperature range, an increase in the NBR content leads to a decrease in the foaming rate which may be due to an increase in the melt viscosity of FRMs in the FRM-0, ..., FRM-20 series (Table 3). The rate-limiting stage of the foaming process is nucleation in the bulk of the liquid phase [6, 42]: gas bubble nuclei are formed in the bulk of the PM during its transition to a viscoelastic flow state with a certain viscosity value. Figure 10 presents the dependence of the foaming rate on the MFI of FRMs at various temperatures.

The results obtained show that the dependence of the foaming rate of FRMs on their MFI is generally linear over the entire temperature range.

The effect of the NBR content in FRMs on the strength of foamed char is of practical interest. As Fig. 11 and Table 3 show, increasing the NBR content in FRMs from 0 to 20% leads to a 4.7-fold increase in the compressive strength of foamed char.

This may be due to the fact that, during the combined pyrolysis of PVC and NBR, the decomposition products of PVC and NBR interact to form condensed compounds. Furthermore, with increasing NBR content, the fraction of low-boiling, low-molecular-weight plasticizer in the PM decreases. This can lead to an increase in thermal stability and a shift in pyrolysis processes toward higher temperatures [43].

As can be seen in Fig. 12 and Table 3, the introduction of NBR alters the pyrolysis process of FRMs in an oxidizing atmosphere.

With an increase in NBR content, the onset degradation temperature of FRMs increases from 222 to 236°C. This is due to the high thermal stability of NBR (280°C). The temperature of the maximum degradation rate at this stage also increases: from 253 to 264°C. Figure 12 shows that at the first stage of degradation, the temperature behavior of all the FRMs considered (dehydrochlorination) is similar. Predominantly NBR pyrolysis occurs in the temperature range of 300–500°C. With an increase in the NBR content

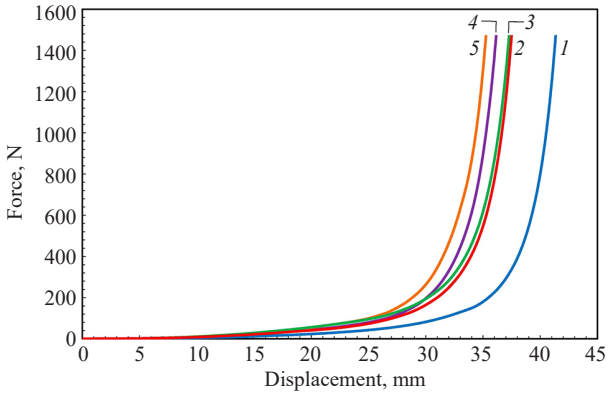

Fig. 11. Compressive load *versus* displacement curves for FRMs with various NBR contents: (*1*) FRM-0, (*2*) FRM-5, (*3*) FRM-10, (*4*) FRM-15, and (*5*) FRM-20

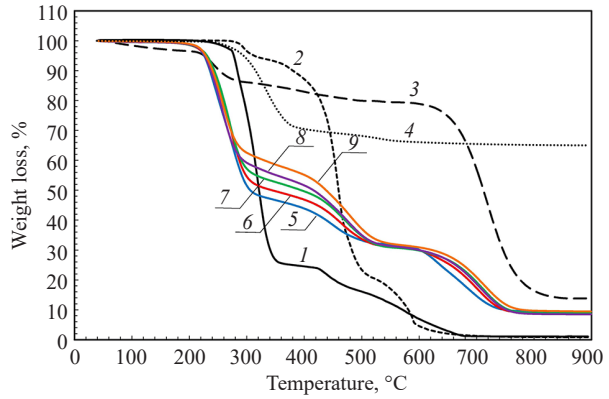

Fig. 12. Weight loss curve of the initial materials and FRM samples in the temperature range of 40–900°C: (*1*) PVC plasticate, (*2*) NBR, (*3*) oxidized graphite, (*4*) aluminium hydroxide, (*5*) FRM-0, (*6*) FRM-5, (*7*) FRM-10, (*8*) FRM-15, and (*9*) FRM-20

in FRMs, the weight loss at this stage increases (from 14.7 to 26.3%). In the temperature range of 600–750°C, foamed graphite in FRMs is oxidized. The presence of NBR leads to a shift of the oxidation process to higher temperatures. The onset oxidation temperature increases from 601°C (for FRM-0) to 659°C (for FRM-20). The NBR content does not significantly affect the residue after oxidation in the temperature range up to 900°C. The content of this residue is in the range of 8.74–9.47%. Also the content of $Al(OH)_3$ in FRMs is 9.88%. Its decomposition occurs according to the equation

$$2Al(OH)_3 \rightarrow Al_2O_3 + 3H_2O.$$

The decomposition gives Al_2O_3 to a content in FRMs of 6.4%. The difference is determined by the non-zero residue left after the oxidation of the expanded graphite in FRMs.

The flammability of the FRMs studied here is not markedly affected by the presence of NBR in them. When tested according to UL-94, all the materials self-extinguish within no more than 1–2 s. This is determined by the high content of fire retardants, primarily oxidized graphite. The established flammability rating for all compositions is V-0.

CONCLUSIONS

The study found that an increase in the fraction of NBR in FRMs results in a decrease in density and hardness (by 2.3 and 10%, respectively), a decrease in tensile strength by 25%, and an increase in elongation by a factor of 2.5. The introduction of fire retardants increases density by an average of 12–25%. It also increases hardness by a factor of 1.3–1.7, and decreases strength and tensile elongation by a factor of 1.8–2.1 and 1.2–1.7, respectively. The investigation of fire-retardant properties showed that an increase in the rubber content causes a decrease in the foaming rate by a factor of 1.43–1.65 in the temperature range from 400 to 800°C. Increasing the rubber content from 0 to 20%

brings about a 16-fold increase in the viscosity of the fire-retardant melt. This affects the foaming rate. It was determined that the foaming rate in the temperature range from 400 to 800°C has a linear dependence on the viscosity of the FRM melt. The addition of rubber increases the strength of foamed char by a factor of 4.8. Thermal analysis demonstrated that increasing the rubber content increases the heat resistance from 222 to 236°C, and the oxidation resistance of expanded graphite in foamed char from 601 to 659°C. The NBR content has no significant effect on the residue after oxidation in the temperature range up to 900°C, with the content of this residue ranging from 8.74 to 9.47%. The presence of NBR in FRMs has no marked effect on flammability. The established flammability rating for all materials is V-0. The results obtained are of great practical interest, since they can be used to predict the optimal composition for producing intumescent FRMs.

Acknowledgments

The study was conducted under the State Assignment of the Lomonosov Moscow State University, project AAAA-A21-121011590086-0.

Authors' contributions

A.A. Galiguzov—conducting experiments, preparing graphic materials, analyzing results, writing individual sections.

N.V. Yashin—writing the introduction, planning the experiments.

V.V. Avdeev—scientific editing, formulating the conclusions.

The authors declare no conflicts of interest.

REFERENCES

1. Zarubina L.P. *Zashchita zdanii, sooruzhenii i konstruktsii ot ognya i shuma. Materialy, tekhnologii, instrumenty i oborudovanie* (*Protection of Buildings, Structures, and Constructions from Fire and Noise. Materials, Technologies, Tools, and Equipment*). Moscow: Infra-Inzheneriya; 2015. P. 7–168 (in Russ.).
2. Focke W.W., Muiambo H., Mhike W., Kruger H.J., Ofosu O. Flexible PVC flame retarded with expandable graphite. *Polym. Degrad. Stab.* 2014;100:63–69. https://doi.org/10.1016/j.polymdegradstab.2013.12.024
3. Qu H., Wu W., Xie J., Xu J. A novel intumescent flame retardant and smoke suppression system for flexible PVC. *Polym. Adv. Technol.* 2011;22(7):1174–1181. https://doi.org/10.1002/pat.1934
4. Khalturinskii N.A., Novikov D.D., Zhorina L.A., Kompaniets L.V., Rudakova T.A. The Effect of the Intumescent F.R. on the Flammability of PVC Plasticates. *Khimicheskaya fizika i mezoskopiya = Chemical Physics and Mesoscopics*. 2009;11(1):22–27 (in Russ.).
5. Galiguzov A.A., Yashin N.V., Avdeev V.V. Thermal stability of fire-retardant materials based on PVC compounds of various compositions. *Plasticheskie massy*. 2023;11-12:21–25 (in Russ.). https://doi.org/10.35164/0554-2901-2023-11-12-21-25
6. Galiguzov A.A., Serdan (jr.) A.A., Yashin N.V., Avdeev V.V. Influence of PVC compound composition on the performance properties and flame retardant efficiency of polymer materials. *Pozharovzryvobezopasnost = Fire and Explosion Safety*. 2023;32(5):26–39 (in Russ.). https://doi.org/10.22227/0869-7493.2023.32.05.26-39

СПИСОК ЛИТЕРАТУРЫ

1. Зарубина Л.П. *Защита зданий, сооружений и конструкций от огня и шума. Материалы, технологии, инструменты и оборудование.* М.: Инфра-Инженерия; 2015. С. 7–168.
2. Focke W.W., Muiambo H., Mhike W., Kruger H.J., Ofosu O. Flexible PVC flame retarded with expandable graphite. *Polym. Degrad. Stab.* 2014;100:63–69. https://doi.org/10.1016/j.polymdegradstab.2013.12.024
3. Qu H., Wu W., Xie J., Xu J. A novel intumescent flame retardant and smoke suppression system for flexible PVC. *Polym. Adv. Technol.* 2011;22(7):1174–1181. https://doi.org/10.1002/pat.1934
4. Халтуринский Н.А., Новиков Д.Д., Жорина Л.А., Компаниец Л.В., Рудакова Т.А. Влияние интумесцентных антипиренов на горючесть ПВХ пластикатов. *Химическая физика и мезоскопия*. 2009;11(1):22–27.
5. Галигузов А.А., Яшин Н.В., Авдеев В.В. Термостойкость огнезащитных материалов на основе ПВХ-пластикатов различного состава. *Пластические массы*. 2023;11-12:21–25. https://doi.org/10.35164/0554-2901-2023-11-12-21-25
6. Галигузов А.А., Сердан (мл.) А.А., Яшин Н.В., Авдеев В.В. Влияние состава ПВХ-пластиката на эксплуатационные свойства и огнезащитную эффективность полимерных материалов на его основе. *Пожаровзрывобезопасность*. 2023;32(5):26–39. https://doi.org/10.22227/0869-7493.2023.32.05.26-39
7. Jimenez M., Duquesne S., Bourbigot S. Multiscale Experimental Approach for Developing High-Performance Intumescent Coatings. *Ind. Eng. Chem. Res.* 2006;45(13):4500–4508. https://doi.org/10.1021/ie060040x

7. Jimenez M., Duquesne S., Bourbigot S. Multiscale Experimental Approach for Developing High-Performance Intumescent Coatings. *Ind. Eng. Chem. Res.* 2006;45(13):4500–4508. https://doi.org/10.1021/ie060040x
8. Biron M. 2-Plastics Overview. In: *A Practical Guide to Plastics Sustainability. Concept, Solutions, and Implementation*. Oxford, UK: Elsevier; 2020. P. 45–85. https://doi.org/10.1016/B978-0-12-821539-5.00002-1
9. Carty P., White S. The effect of DOP plasticizer on smoke formation in poly(vinyl chloride). *Polymer*.1992;33(5): 1110–1111. https://doi.org/10.1016/0032-3861(92)90033-S
10. Tüzüm Demir A.P., Ulutan S. Migration of phthalate and non-phthalate plasticizers out of plasticized PVC films into air. *J. Appl. Polym. Sci*. 2013;128(3):1948–1961. https://doi.org/10.1002/app.38291
11. Lavrov N.A., Belukhichev E.V. Polyvinyl chloride-based polymer blends (overview). *Plasticheskie massy*. 2020;3-4:55–59 (in Russ.). https://doi.org/10.35164/0554-2901-2020-3-4-55-59
12. George K.E., Joseph R., Francis D.J. Studies on NBR/PVC blends. *J. Appl. Polym. Sci*. 1986;32(1):2867–2873. https://doi.org/10.1002/APP.1986.070320102
13. Milner P.W. Modification of PVC with NBR. In: Whelan A., Goff J.P. (Eds.) *Developments in Plastics Technology-4*. Dordrecht, NL: Springer; 1989. P. 99–137. https://doi.org/10.1007/978-94-009-1101-7_3
14. Xiaojiang Z., Pu H.H., Yafei L. Morphology and properties of blended NBR/PVC/BR elastomers. *J. Polym. Sci. Part C: Polymer Letters*. 1988;26(6):255–258. https://doi.org/10.1002/pol.1988.140260601
15. Thomas N.L., Harvey R.J. PVC/nitrile rubber blends. *Prog. Rubber Plast. Tech*. 2001;17(1):1–12. https://doi.org/10.1177/147776060101700101
16. Perera M.C.S., Ishiaku U.S., Ishak Z.A.M. Thermal degradation of PVC/NBR and PVC/ENR50 binary blends and PVC/ENR50/NBR ternary blends studied by DMA and solid state NMR. *Polym. Degrad. Stab*. 2000;68(3):393–402. https://doi.org/10.1016/S0141-3910(00)00024-0
17. Zakrzewski G.A. Investigation of the compatibility of butadiene—acrylonitrile copolymers with poly(vinyl chloride). *Polymer*. 1973;14(8):347–351. https://doi.org/10.1016/0032-3861(73)90018-9
18. Alneamah M., Almaamori M. Study of Thermal Stability of Nitrile Rubber/Polyimide Compounds. *Int. J. Mater. Chem*. 2015;5(1):1–3. https://doi.org/10.5923/j.ijmc.20150501.01
19. Levine Y., Chetrit E., Fishman Y., Siyum Y., Rabaev M., Fletcher A., Tartakovsky K. A novel approach to plasticizer content calculation in an acrylonitrile-butadiene rubber real-time aging study (NBR). *Polym. Test*. 2023;124:108091. https://doi.org/10.1016/j.polymertesting.2023.108091
20. Pappa A., Mikedi K., Agapiou A., Karma S., Pallis G.C., Statheropoulos M., Burke M. TG–MS analysis of nitrile butadiene rubber blends (NBR/PVC). *J. Anal. Appl. Pyrolysis*. 2011;92(1):106–110. https://doi.org/10.1016/j.jaap.2011.05.003
21. Choi S.-S., Han D.-H. Pyrolysis behaviors of poly(acrylonitrile-*co*-butadiene) with differing microstructures. *J. Anal. Appl. Pyrolysis*. 2007;80(1):53–60. https://doi.org/10.1016/j.jaap.2006.12.032
22. Yu J., Sun L., Ma C., Qiao Y., Yao H. Thermal degradation of PVC: A review. *Waste Manag*. 2016;48:300–314. https://doi.org/10.1016/j.wasman.2015.11.041
23. Marcilla A., García J.C., Beltrán M. 9 – Plasticization Steps. In: Wypych G. (Ed.) *Handbook of Plasticizers*. Toronto: ChemTec Publishing; 2017. P. 195–208. https://doi.org/10.1016/B978-1-895198-97-3.50011-1

8. Biron M. 2-Plastics Overview. In: *A Practical Guide to Plastics Sustainability. Concept, Solutions, and Implementation*. Oxford, UK: Elsevier; 2020. P. 45–85. https://doi.org/10.1016/B978-0-12-821539-5.00002-1
9. Carty P., White S. The effect of DOP plasticizer on smoke formation in poly(vinyl chloride). *Polymer*.1992;33(5): 1110–1111. https://doi.org/10.1016/0032-3861(92)90033-S
10. Tüzüm Demir A.P., Ulutan S. Migration of phthalate and non-phthalate plasticizers out of plasticized PVC films into air. *J. Appl. Polym. Sci*. 2013;128(3):1948–1961. https://doi.org/10.1002/app.38291
11. Лавров Н.А., Белухичев Е.В. Полимерные смеси на основе поливинилхлорида (обзор). *Пластические массы*. 2020;3-4: 55–59. https://doi.org/10.35164/0554-2901-2020-3-4-55-59
12. George K.E., Joseph R., Francis D.J. Studies on NBR/PVC blends. *J. Appl. Polym. Sci*. 1986;32(1):2867–2873. https://doi.org/10.1002/APP.1986.070320102
13. Milner P.W. Modification of PVC with NBR. In: Whelan A., Goff J.P. (Eds.) *Developments in Plastics Technology-4*. Dordrecht, NL: Springer; 1989. P. 99–137. https://doi.org/10.1007/978-94-009-1101-7_3
14. Xiaojiang Z., Pu H.H., Yafei L. Morphology and properties of blended NBR/PVC/BR elastomers. *J. Polym. Sci. Part C: Polymer Letters*. 1988;26(6):255–258. https://doi.org/10.1002/pol.1988.140260601
15. Thomas N.L., Harvey R.J. PVC/nitrile rubber blends. *Prog. Rubber Plast. Tech*. 2001;17(1):1–12. https://doi.org/10.1177/147776060101700101
16. Perera M.C.S., Ishiaku U.S., Ishak Z.A.M. Thermal degradation of PVC/NBR and PVC/ENR50 binary blends and PVC/ENR50/NBR ternary blends studied by DMA and solid state NMR. *Polym. Degrad. Stab*. 2000;68(3):393–402. https://doi.org/10.1016/S0141-3910(00)00024-0
17. Zakrzewski G.A. Investigation of the compatibility of butadiene—acrylonitrile copolymers with poly(vinyl chloride). *Polymer*. 1973;14(8):347–351. https://doi.org/10.1016/0032-3861(73)90018-9
18. Alneamah M., Almaamori M. Study of Thermal Stability of Nitrile Rubber/Polyimide Compounds. *Int. J. Mater. Chem*. 2015;5(1):1–3. https://doi.org/10.5923/j.ijmc.20150501.01
19. Levine Y., Chetrit E., Fishman Y., Siyum Y., Rabaev M., Fletcher A., Tartakovsky K. A novel approach to plasticizer content calculation in an acrylonitrile-butadiene rubber real-time aging study (NBR). *Polym. Test*. 2023;124:108091. https://doi.org/10.1016/j.polymertesting.2023.108091
20. Pappa A., Mikedi K., Agapiou A., Karma S., Pallis G.C., Statheropoulos M., Burke M. TG–MS analysis of nitrile butadiene rubber blends (NBR/PVC). *J. Anal. Appl. Pyrolysis*. 2011;92(1):106–110. https://doi.org/10.1016/j.jaap.2011.05.003
21. Choi S.-S., Han D.-H. Pyrolysis behaviors of poly(acrylonitrile-*co*-butadiene) with differing microstructures. *J. Anal. Appl. Pyrolysis*. 2007;80(1):53–60. https://doi.org/10.1016/j.jaap.2006.12.032
22. Yu J., Sun L., Ma C., Qiao Y., Yao H. Thermal degradation of PVC: A review. *Waste Manag*. 2016;48:300–314. https://doi.org/10.1016/j.wasman.2015.11.041
23. Marcilla A., García J.C., Beltrán M. 9 – Plasticization Steps. In: Wypych G. (Ed.) *Handbook of Plasticizers*. Toronto: ChemTec Publishing; 2017. P. 195–208. https://doi.org/10.1016/B978-1-895198-97-3.50011-1
24. Khoshnoud P., Abu-Zahra N. Kinetics of thermal decomposition of PVC/fly ash composites. *Int. J. Polym. Anal. Ch*. 2017;23(2): 170–80. https://doi.org/10.1080/1023666X.2017.1404668
25. Ye L., Li T., Hong L. Understanding enhanced char formation in the thermal decomposition of PVC resin: Role of intermolecular chlorine loss. *Mater. Today Commun*. 2021;26:102186. https://doi.org/10.1016/j.mtcomm.2021.102186

24. Khoshnoud P., Abu-Zahra N. Kinetics of thermal decomposition of PVC/fly ash composites. *Int. J. Polym. Anal. Ch*. 2017;23(2):170–80. https://doi.org/10.1080/1023666X.2017.1404668
25. Ye L., Li T., Hong L. Understanding enhanced char formation in the thermal decomposition of PVC resin: Role of intermolecular chlorine loss. *Mater. Today Commun*. 2021;26:102186. https://doi.org/10.1016/j.mtcomm.2021.102186
26. Galiguzov A.A., Yashin N.V., Avdeev V.V. Thermal properties of materials based on ethylene vinyl acetate and various flame retardants during thermal oxidative degradation. *Plasticheskie massy.* 2024;5:3–10 (in Russ.). https://doi.org/10.35164/0554-2901-2024-05-3-10
27. Inagaki M., Tashiro R., Washino Y., Toyoda M. Exfoliation process of graphite via intercalation compounds with sulfuric acid. *J. Phys. Chem. Solids*. 2004;65(2-3):133–137. https://doi.org/10.1016/j.jpcs.2003.10.007
28. Arogundade A.I., Megat-Yussof P.S.M., Afolabi L.O. Evaluation of compression strength of intumescent char using ASTM 1162 00. *J. Coat. Technol. Res*. 2021;18:935–943. https://doi.org/10.1007/s11998-020-00434-0
29. Pan N., Guan D., He T., Wang R., Wyman I., Jin Y., Xia C. Removal of Th^{4+} ions from aqueous solutions by graphene oxide. *J. Radioanal. Nucl. Chem.* 2013;298:1999–2008. https://doi.org/10.1007/s10967-013-2660-2
30. Salvatore M., Carotenuto G., De Nicola S., Camerlingo C., Ambrogi V., Carfagna C. Synthesis and Characterization of Highly Intercalated Graphite Bisulfate. *Nanoscale Res. Lett.* 2017;12:167. https://doi.org/10.1186/s11671-017-1930-2
31. Rimkute G., Gudaitis M., Barkauskas J., Zarkov A., Niaura G., Gaidukevic J. Synthesis and Characterization of Graphite Intercalation Compounds with Sulfuric Acid. *Crystals.* 2022;12(3):421. https://doi.org/10.3390/cryst12030421
32. Madejová J., Gates W.P., Petit S. 5 – IR Spectra of Clay Minerals. In: Zhuang G., Yuan P. (Eds.) *Developments in Clay Science.* Oxford, UK: Elsevier; 2017. V. 8. P. 107–149. https://doi.org/10.1016/B978-0-08-100355-8.00005-9
33. Srinivasan S., Valsadwala A.S., Karthik D., Suganandam D., Begum S.S. A Comparative Study on the Characteristics of Crumb Rubber with Commercial Rubbers. In: Ganippa L., Karthikeyan R., Muralidharan V. (Eds.) *Advances in Design and Thermal Systems. Lecture Notes in Mechanical Engineering*. Singapore: Springer Nature Singapore Pte Ltd; 2021. P. 213–220. https://doi.org/10.1007/978-981-33-6428-8_15
34. Deanin R.D., Normandin R.O., Patel G.J. 13 – Filler Reinforcement of Plasticized Poly(vinyl chloride). In: Deanin R.D., Schott N.R. (Eds.). *Fillers and Reinforcements for Plastics*. York, PA, USA: The Maple Press Co.; 1974. P. 128–136. https://doi.org/10.1021/ba-1974-0134.ch013
35. Glazkov S.S. A model of thermodynamic compatibility of the filler with the polymeric matrix in a composite. *Russ. J. Appl. Chem*. 2007;80(9):1594–1597. https://doi.org/10.1134/S1070427207090297 [Original Russian Text: Glazkov S.S. A model of thermodynamic compatibility of the filler with the polymeric matrix in a composite. *Zhurnal prikladnoi khimii.* 2007;80(9):1562–1567 (in Russ.). https://elibrary.ru/iccmfz]
36. Huang X.D., Goh S.H. Miscibility of C60-end-capped poly(ethylene oxide) with poly(vinyl chloride). *Polymer*. 2002;43(4): 1417–1421. https://doi.org/10.1016/S0032-3861(01)00705-4
37. Guler S.H., Simsek T., Guler O., Dikici B. Possible Interaction of PVC with Micro-and Nano-fillers. In: Akhina H., Sabu T. (Eds.). *Poly(Vinyl Chloride) Based Composites and Nanocomposites. Engineering Materials.* Cham, GER: Springer; 2024. P. 335–360. https://doi.org/10.1007/978-3-031-45375-5_16
26. Галигузов А.А., Яшин Н.В., Авдеев В.В. Термические свойства материалов на основе этиленвинилацетата и различных антипиренов при термоокислительном разложении. *Пластические массы.* 2024;5:3–10. https://doi.org/10.35164/0554-2901-2024-05-3-10
27. Inagaki M., Tashiro R., Washino Y., Toyoda M. Exfoliation process of graphite via intercalation compounds with sulfuric acid. *J. Phys. Chem. Solids*. 2004;65(2-3):133–137. https://doi.org/10.1016/j.jpcs.2003.10.007
28. Arogundade A.I., Megat-Yussof P.S.M., Afolabi L.O. Evaluation of compression strength of intumescent char using ASTM 1162 00. *J. Coat. Technol. Res*. 2021;18:935–943. https://doi.org/10.1007/s11998-020-00434-0
29. Pan N., Guan D., He T., Wang R., Wyman I., Jin Y., Xia C. Removal of Th^{4+} ions from aqueous solutions by graphene oxide. *J. Radioanal. Nucl. Chem.* 2013;298:1999–2008. https://doi.org/10.1007/s10967-013-2660-2
30. Salvatore M., Carotenuto G., De Nicola S., Camerlingo C., Ambrogi V., Carfagna C. Synthesis and Characterization of Highly Intercalated Graphite Bisulfate. *Nanoscale Res. Lett.* 2017;12:167. https://doi.org/10.1186/s11671-017-1930-2
31. Rimkute G., Gudaitis M., Barkauskas J., Zarkov A., Niaura G., Gaidukevic J. Synthesis and Characterization of Graphite Intercalation Compounds with Sulfuric Acid. *Crystals.* 2022;12(3):421. https://doi.org/10.3390/cryst12030421
32. Madejová J., Gates W.P., Petit S. 5 – IR Spectra of Clay Minerals. In: Zhuang G., Yuan P. (Eds.) *Developments in Clay Science.* Oxford, UK: Elsevier; 2017. V. 8. P. 107–149. https://doi.org/10.1016/B978-0-08-100355-8.00005-9
33. Srinivasan S., Valsadwala A.S., Karthik D., Suganandam D., Begum S.S. A Comparative Study on the Characteristics of Crumb Rubber with Commercial Rubbers. In: Ganippa L., Karthikeyan R., Muralidharan V. (Eds.) *Advances in Design and Thermal Systems. Lecture Notes in Mechanical Engineering*. Singapore: Springer Nature Singapore Pte Ltd; 2021. P. 213–220. https://doi.org/10.1007/978-981-33-6428-8_15
34. Deanin R.D., Normandin R.O., Patel G.J. 13 – Filler Reinforcement of Plasticized Poly(vinyl chloride). In: Deanin R.D., Schott N.R. (Eds.). *Fillers and Reinforcements for Plastics*. York, PA, USA: The Maple Press Co.; 1974. P. 128–136. https://doi.org/10.1021/ba-1974-0134.ch013
35. Глазков С.С. Модель термодинамической совместимости наполнителя и полимерной матрицы в композите. *Журн. прикладной химии*. 2007;80(9):1562–1567. https://elibrary.ru/iccmfz
36. Huang X.D., Goh S.H. Miscibility of C60-end-capped poly(ethylene oxide) with poly(vinyl chloride). *Polymer*. 2002;43(4): 1417–1421. https://doi.org/10.1016/S0032-3861(01)00705-4
37. Guler S.H., Simsek T., Guler O., Dikici B. Possible Interaction of PVC with Micro-and Nano-fillers. In: Akhina H., Sabu T. (Eds.). *Poly(Vinyl Chloride) Based Composites and Nanocomposites. Engineering Materials.* Cham, GER: Springer; 2024. P. 335–360. https://doi.org/10.1007/978-3-031-45375-5_16
38. Lu Y., Jiang N., Li X., Xu S. Effect of inorganic-organic surface modification of calcium sulfate whiskers on mechanical and thermal properties of calcium sulfate whisker/poly(vinyl chloride) composites. *RSC Adv*. 2017;7(73):46486–46498. https://doi.org/10.1039/C7RA09193A
39. Sato Y., Furakawa J. A molecular theory of filler reinforcement based upon the conception of internal deformation (a rough approximation of the internal deformation). *Rubber Chem. Technol.* 1963;36(4):1081–1106. https://doi.org/10.5254/1.3539632
40. Серенко О.А., Насруллаев И.Н., Баженов С.Л. Деформационные свойства полиэтилена средней плотности, наполненного частицами резины. *Высокомолекулярные соединения. Серия А.* 2003;45(5):759–766. https://elibrary.ru/oojlwj

38. Lu Y., Jiang N., Li X., Xu S. Effect of inorganic-organic surface modification of calcium sulfate whiskers on mechanical and thermal properties of calcium sulfate whisker/poly(vinyl chloride) composites. *RSC Adv.* 2017;7(73):46486–46498. https://doi.org/10.1039/C7RA09193A
39. Sato Y., Furakawa J. A molecular theory of filler reinforcement based upon the conception of internal deformation (a rough approximation of the internal deformation). *Rubber Chem. Technol.* 1963;36(4):1081–1106. https://doi.org/10.5254/1.3539632
40. Serenko O.A., Nasrullaev I.N., Bazhenov S.L. The stress-strain properties of medium-density polyethylene filled with rubber particles. *Polym. Sci. Ser. A.* 2003;45(5):450–455. https://elibrary.ru/libasv
[Original Russian Text: Serenko O.A., Nasrullaev I.N., Bazhenov S.L. The stress-strain properties of medium-density polyethylene filled with rubber particles. *Vysokomolekulyarnye soedineniya. Seriya A.* 2003;45(5):759–766 (in Russ.). https://elibrary.ru/oojlwj]
41. Serenko O.A., Bazhenov S.L., Nasrullaev I.N., Berlin A.A. The effect of particle dimensions on the shape of formed defects in a particulate filled composite. *Polym. Sci. Ser. A.* 2005;47(1):49–56. https://elibrary.ru/ljaxth
[Original Russian Text: Serenko O.A., Bazhenov S.L., Nasrullaev I.N., Berlin A.A. The effect of particle dimensions on the shape of formed defects in a particulate filled composite. *Vysokomolekulyarnye soedineniya. Seriya A.* 2005;47(1):64–72 (in Russ.). https://elibrary.ru/hsafln]
42. Arkhangelsky I.V., Godunov I.A., Yashin N.V., Naganovskii Yu.K., Shornikova O.N. The kinetics of intumescent flame retardant foaming. *Pozharovzryvobezopasnost = Fire and Explosion Safety.* 2020;29(5):71–81 (in Russ.). https://doi.org/10.22227/PVB.2020.29.05.71-81
43. Pruneda F., Suñol J., Andreu-Mateu F., Colom X. Thermal characterization of nitrile butadiene rubber (NBR)/PVC blends. *J. Therm. Anal. Calorim.* 2005;80:187–190. https://doi.org/10.1007/s10973-005-0634-5
41. Серенко О.А., Баженов С.Л., Насруллаев И.Н., Берлин А.А. Влияние размера частиц на форму образующихся дефектов в дисперсно наполненном композите. *Высокомолекулярные соединения. Серия А.* 2005;47(1):64–72. https://elibrary.ru/hsafln
42. Архангельский И.В., Годунов И.А., Яшин Н.В., Нагановский Ю.К., Шорникова О.Н. Кинетика вспенивания терморасширяющихся огнезащитных составов. *Пожаровзрывобезопасность.* 2020;29(5):71–81. https://doi.org/10.22227/PVB.2020.29.05.71-81
43. Pruneda F., Suñol J., Andreu-Mateu F., Colom X. Thermal characterization of nitrile butadiene rubber (NBR)/PVC blends. *J. Therm. Anal. Calorim.* 2005;80:187–190. https://doi.org/10.1007/s10973-005-0634-5

About the Authors

Andrey A. Galiguzov, Junior Researcher, Department of Chemical Technology and New Materials, Faculty of Chemistry, Lomonosov Moscow State University (1/11, Leninskie Gory, Moscow, 119991, Russia). E-mail: agaliguzov@yandex.ru. Scopus Author ID 55362650300, RSCI SPIN-code 4148-9040, https://orcid.org/0000-0002-5675-3891

Nikolay V. Yashin, Dr. Sci. (Chem.), Senior Researcher, Department of Chemical Technology and New Materials, Faculty of Chemistry, Lomonosov Moscow State University (1/11, Leninskie Gory, Moscow, 119991, Russia). E-mail: yashin.ni.v@gmail.com. Scopus Author ID 6602800878, ResearcherID D-8087-2015, RSCI SPIN-code 3248-5409, https://orcid.org/0000-0002-2232-8192

Viktor V. Avdeev, Dr. Sci. (Chem.), Professor, Head of the Department of Chemical Technology and New Materials, Faculty of Chemistry, Lomonosov Moscow State University (1/11, Leninskie Gory, Moscow, 119991, Russia). E-mail: avdeev@highp.chem.msu.ru. Scopus Author ID 7005990761, https://orcid.org/0000-0001-5573-2987

Об авторах

Галигузов Андрей Анатольевич, младший научный сотрудник, кафедра химической технологии и новых материалов, Химический факультет, Московский государственный университет им. М.В. Ломоносова (119991, Россия, Москва, Ленинские горы, д. 1, стр. 11). E-mail: agaliguzov@yandex.ru. Scopus Author ID 55362650300, SPIN-код РИНЦ 4148-9040, https://orcid.org/0000-0002-5675-3891

Яшин Николай Владимирович, д.х.н., старший научный сотрудник, кафедра химической технологии и новых материалов, Химический факультет, Московский государственный университет им. М.В. Ломоносова (119991, Россия, Москва, Ленинские горы, д. 1, стр. 11). E-mail: yashin.ni.v@gmail.com. Scopus Author ID 6602800878, ResearcherID D-8087-2015, SPIN-код РИНЦ 3248-5409, https://orcid.org/0000-0002-2232-8192

Авдеев Виктор Васильевич, д.х.н., профессор, заведующий кафедрой химической технологии и новых материалов, Химический факультет, Московский государственный университет им. М.В. Ломоносова (119991, Россия, Москва, Ленинские горы, д. 1, стр. 11). E-mail: avdeev@highp.chem.msu.ru. Scopus Author ID 7005990761, https://orcid.org/0000-0001-5573-2987

Translated from Russian into English by V. Glyanchenko
Edited for English language and spelling by Dr. David Mossop